

## 2. Simple Performance Estimation

### 2.1 Important Performance Parameters

UAV performance parameters of interest may include stall speed, climb rate, maximum altitude, range, maximum speed, maximum sustained turn rates, and many other flight characteristics that depend on the UAV intended use. These, in turn are determined by the aircraft weight, propulsion system performance and the vehicle's aerodynamic characteristics.

At the earliest stages of UAV conceptual design, some estimate of weight, propulsive power and efficiency, and aerodynamic performance is required. Unlike transport aircraft, simple parametric models are often not available and custom methods are common. Techniques for estimating these characteristics are described briefly in the following sections and in the AA241A,B notes:

(<http://adg.stanford.edu/aa241/aircraftdesign.html>)

Once these characteristics are known, or estimated, some of the basic performance measures can be computed directly. These include the following

#### **Stall speed**

For transport aircraft, stalling speed is primarily constrained by runway length requirements. One might think that since the field length requirements for UAV's may not be critical constraints (although that's not always true), that stalling speed is not an issue, but there are several reasons that it might be. If the UAV is to land on rough fields, reducing the stall speed can reduce the likelihood of damage and stalling speed affects gear design on some large UAV's. Stalling speed may also have a direct effect on the ability to maneuver – especially important for combat UAV's. But for high altitude and long endurance UAV's making sure that the stalling speed is sufficiently low to achieve the desired design condition is often critical.

$$V_{stall} = \sqrt{\frac{2W}{S\rho C_{Lmax}}}$$

where W is the vehicle weight, S is the wing reference area,  $C_{Lmax}$  is the maximum lift coefficient, and  $\rho$  is the air density (see <http://desktopaero.com/stdatm.html> or the AA241 A,B notes).

As can quickly be shown (by assuming a quadratic drag polar as mentioned in the following sections), the lift coefficient for maximum lift-to-drag ratio (closely related to that for maximum range is:

$$C_{L|L/D_{max}} = \sqrt{\pi AR C_{Dp}}$$

while the lift coefficient for maximum endurance (assuming fixed propulsion efficiency and quadratic polar) is:

$$C_{L|L/D_{max}} = \sqrt{3\pi AR C_{Dp}}$$

The point here is that for airplanes with high AR (span<sup>2</sup> / S), required for long endurance high altitude flight, this  $C_L$  can easily exceed the maximum  $C_L$  of the wing. The situation is made worse for low Reynolds number aircraft for which  $C_{Dp}$  is higher and  $C_{Lmax}$  lower.

### Endurance

If the efficiency of the propulsion systems is known and the total energy content of the fuel or battery is given, the endurance may be estimated based on energy considerations. For battery-powered aircraft the weight of the airplane does not vary in time, so the endurance may be easily estimated. The power required for level flight is:  $P = D V$

In this case, the drag may be computed as described in the following sections with the substitution that Lift  $\approx$  Weight.

This power is the that delivered by the propulsion system to overcome drag. However, the power that is delivered to the motor must be converted to mechanical work, may go through a gear box, and may be converted into thrust through a propeller. All of these processes introduce some loss so that the actual power required by the motor is:

$$P_{req} = \frac{DV}{\eta_{overall}}$$

The total energy used to overcome drag is then:

$E_{req} = D V t$ , where  $t$  is the endurance.

If the energy available from the batteries is  $E_{avail}$ , and the efficiency of the motor and propellers is  $\eta_{overall}$ , then the endurance may be written in terms of the energy in the batteries:

$$t = \frac{E_{avail} \eta_{overall}}{DV}$$

If the overall propulsion system efficiency is constant with speed (it's usually not), then the endurance is maximized by minimizing  $D V$ . Otherwise, it requires that the propulsion system (e.g. propeller) and airframe are optimized together. Clearly the speed

for maximum endurance is not the same as the speed for minimum drag (unless the efficiency varies in a special way). While the range of an aircraft with fixed propulsive efficiency is maximum when the drag is minimum (and  $L/D$  is maximum), the endurance generally occurs at a lower speed (or higher  $C_L$ ).

### Ceiling

Since the power required for level flight increases as speed increases, the airplane ceiling may be limited by the available power. This is because the airplane speed varies with density:

$$V = \sqrt{\frac{2W}{S\rho C_L}}$$

It is also common that the maximum power available from the engine decreases with altitude. This is certainly true of internal combustion engines, but one of the features of electric propulsion is that the available (engine) power changes little with altitude. The propeller performance does change with altitude and it is important to evaluate this at some point in the early stages of the aircraft design.

The ceiling may also be limited, not by power, but by total energy. Since the climb rate varies with altitude, one must integrate the motion of the airplane over time to determine the maximum achievable altitude.

### Climb Rate

The rate of climb may be determined from energy considerations. The rate at which power is being used by the system is that due to changing the energy of the system and the rate at which drag is consuming the power. In the case that the climb angle is not large, the drag may still be computed by assuming that the lift is approximately equal to the weight, but the rate of energy use is given by:

$$P_{req} \eta_{overall} = TV = VD + W\dot{h}$$

or:

$$\dot{h} = \frac{V(T - D)}{W}$$

This assumes that the speed is constant. If the airplane is accelerating (as it would if the  $C_L$  were constant and the density were decreasing with altitude), there is an additional term associated with the kinetic energy gain.

When density, weight, available power, or speed vary during the flight, the climb rate changes and a more accurate estimate of the altitude is obtained by integrating the performance in time. This kind of complete "mission analysis" is common even in the early stages of UAV design.

## 2.2 Initial Weight Estimation

For AA241X, the most reasonable approach to obtain a rough estimate of your aircraft weight is to create a weight statement that lists all of the components whose weights you know, whose weights you estimate, and whose weights you can compute by some means. In this class the propulsion system and battery weight is given; the control system weight is known, and you must estimate the fuselage, tail, and wing weights. The latter you can do parametrically, knowing the density of foam, estimating airfoil thickness, and making a rough estimate of the weight of skins, stiffeners, control surface hinges, etc..

a241bweights.xls									
	A	B	C	D	E	F	G	H	I
1	<b>AA241 Airplane Weight Statement</b>								
2	(all masses in g)								
3		Current	Guess / Est.	Statistics/Calc.	Vendor Spec	Measured	Comment		
4	battery	64	65	50	60	64		8 cell 370mah NMH	
5	motor and prop	29	36	36	30	29		2 GWS EDP-20	
6	speed ctrl	6	6	6	6	6		GWS	
7	receiver	9	9	9	9	9		Feather	
8	servos (2)	10	10	10	8	10		Cirrus 4	
9	subtotal ctrl&pwr	118	126	111	113	118			
10									
11	airframe	162	200	107					
12									
13	wing	75	75	75					
14	tails	10	10	10					
15	booms	13	13	13					
16	pod	9	9	9					
17									
18									
19	total	280	326	218	113				

Note that parametric weight estimation based on large aircraft data is usually very inappropriate for small UAV design. Even the form of the variation of wing weight with size may be quite different.

## 2.3 Initial Propulsion System Performance


As indicated previously, the propulsion system performance is critical to the performance of the vehicle. Two major parameters are of particular interest: the maximum available thrust or power and the system efficiency. The thrust, efficiency, speed, and power into the motor are related by:

$$P_{\text{into motor}} = T V / \eta_{\text{overall}}$$

The overall efficiency is the product of the component efficiencies of the motor, control electronics, gear box, and propeller. These parameters may be computed using computational analysis models of the components or may be based on experimental data. A detailed analysis includes the effect of load and RPM on the motor efficiency and the effect of speed and RPM on propeller efficiency.

However, if one assumes that the propeller and motor are well matched to the design flight condition, some simple estimates of over efficiency are possible. For very good brushless motors one might achieve motor efficiencies as high as much as 90%. For small brushed motors 50% is very common and 25% not rare. With this large variation, it is essential to have data on a particular motor. Similarly, well-designed propellers may reach efficiencies of 85%, but small direct-drive props at low Reynolds numbers are more commonly about 50% efficient. Motor control electronics similarly range in performance with 60% to 90% variation seen.

Propeller performance is often characterized by curves that illustrate the variation of thrust and torque with RPM, forward speed, and sometimes pitch angle. Motor performance is often described by similar curves and is also summarized with a few parameters such as maximum no load RPM and current and stall torque and current. From just these four numbers a simple motor performance map may be created.



GW/EDP-50XC (EP3020)

- ☒ ITEM : GW/EDP-50XC
- ☒ MOTOR : CN12RXC
- ☒ WEIGHT : 15g (0.53 oz)
- ☒ W/CB MOTOR \* 1, EP3020 PROPELLER\* 2

PROPELLER	Volts (v)	Amps (A)	Thrust		Power (w)	Efficiency	
			(g)	(oz)		(g/w)	(oz/kw)
EP3020	6.0	1.35	51	1.80	8.10	6.30	222
EP3020	7.2	1.66	60	2.10	11.95	5.02	177

The final critical element of an electric propulsion system is the source of electrical power. In AA241X we will provide a standard battery pack, but in general one must examine battery total energy, maximum power output, and weight and match these to the needs of the rest of the propulsion system.

## 2.4 Drag Bookkeeping

For low speed aircraft we divide drag into the following components:

**Drag = Skin Friction Drag + Viscous Pressure Drag + Inviscid (Vortex) Drag**

The first two effects are often combined into a single term called parasite drag.

*Skin Friction* drag arises from the shearing stresses at the surface of a body due to viscosity. It accounts for most of the drag of a transport aircraft in cruise.

*Viscous pressure drag* also is produced by viscous effects, but not so directly. The pressure distribution is modified by the presence of a boundary layer. Although in 2-D inviscid flow the pressures on forward and aft surfaces balance so that no drag is produced, the effect of the boundary layer leads to an imperfect canceling of these pressures so some additional drag is created.

*Inviscid or vortex drag* is produced by the trailing vortex wake of a three-dimensional lifting system.

The parasite drag may be estimated as:

Drag = Skin friction and pressure drag + Lift-Dependent Viscous Drag + Vortex Drag

The drag is often expressed in dimensionless form:

$$C_D = \frac{\text{Drag}}{\frac{\rho}{2} V^2 S_{\text{ref}}}$$

where  $S_{\text{ref}}$  is the reference area. The reference area is not so clear when the wing is not a simple tapered planform, but for the purposes of this class, it is taken to be the projected area of the equivalent trapezoidal wing planform. The parasite drag is often written in terms of the equivalent flat plate drag area,  $f$ :

$$f = C_{D_p} S_{\text{ref}} = \frac{\text{Parasite Drag}}{\frac{\rho}{2} V^2}$$

If one assumes that the vortex drag varies with  $C_L^2$  and the parasite drag is constant with  $C_L$ , the overall drag may be written:

$$C_D = C_{D_p} + \frac{C_L^2}{\pi A R e} \quad \text{or in dimensional form:} \quad D = qf + \frac{L^2}{q \pi b^2 e}$$

## 2.4.1 Parasite Drag

The parasite drag of a typical airplane in the cruise configuration consists primarily of the skin friction, roughness, and pressure drag of the major components. There is usually some additional parasite drag due to such things as fuselage upsweep, control surface gaps, base areas, and other extraneous items. Since most of the elements that make up the total parasite drag are dependent on Reynolds number and since some are dependent on Mach number, it is necessary to specify the conditions under which the parasite drag is to be evaluated. In the method of these notes, the conditions selected are 0.5 Mach number and the Reynolds number corresponding to the flight condition of interest.

The basic parasite drag area for airfoil and body shapes can be computed from the following expression:

$$f = k c_f S_{wet}$$

where the skin friction coefficient,  $c_f$ , which is based on the exposed wetted area includes the effects of roughness, and the form factor,  $k$ , accounts for the effects of both superelevations and pressure drag.  $S_{wet}$  is the total wetted area of the body or surface.

Computation of the overall parasite drag requires that we compute the drag area of each of the major components (fuselage, wing, nacelles and pylons, and tail surfaces) and then evaluate the additional parasite drag components described above.

We thus write:

$$C_{Dp} = \sum k_i c_{fi} S_{weti} / S_{ref}$$

where the sum includes skin friction, and pressure drag at zero lift of the major components.  $c_{fi}$  is the average skin friction coefficient for a rough plate with transition at flight Reynolds number. Equivalent roughness is determined from flight test data.

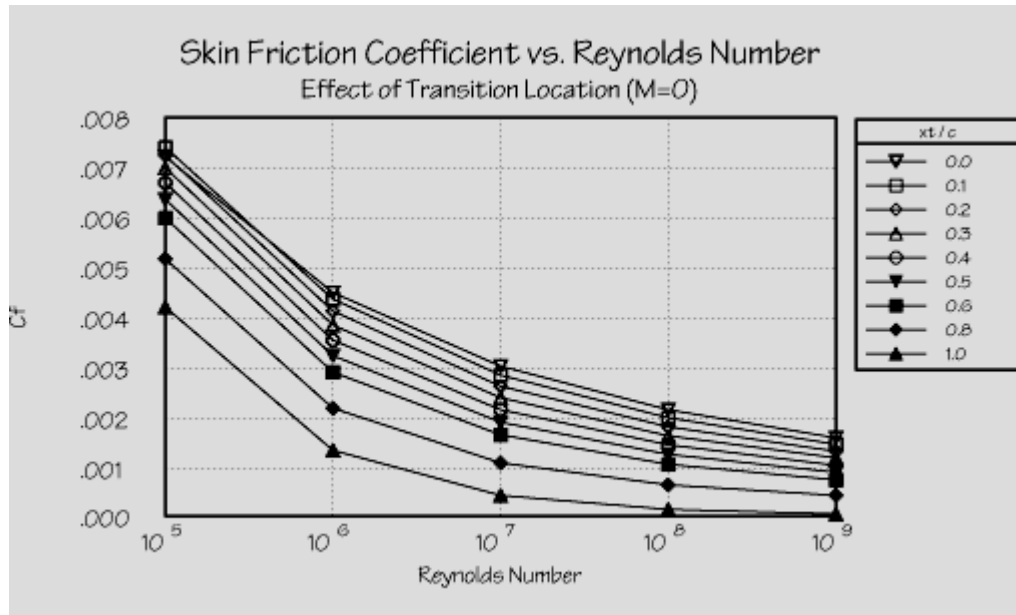
These computations are divided into evaluation of the following terms:

- [Skin friction coefficient,  \$c\_f\$](#)
- [Form factor,  \$k\$](#)
- [Wetted area,  \$S\_{wet}\$](#)

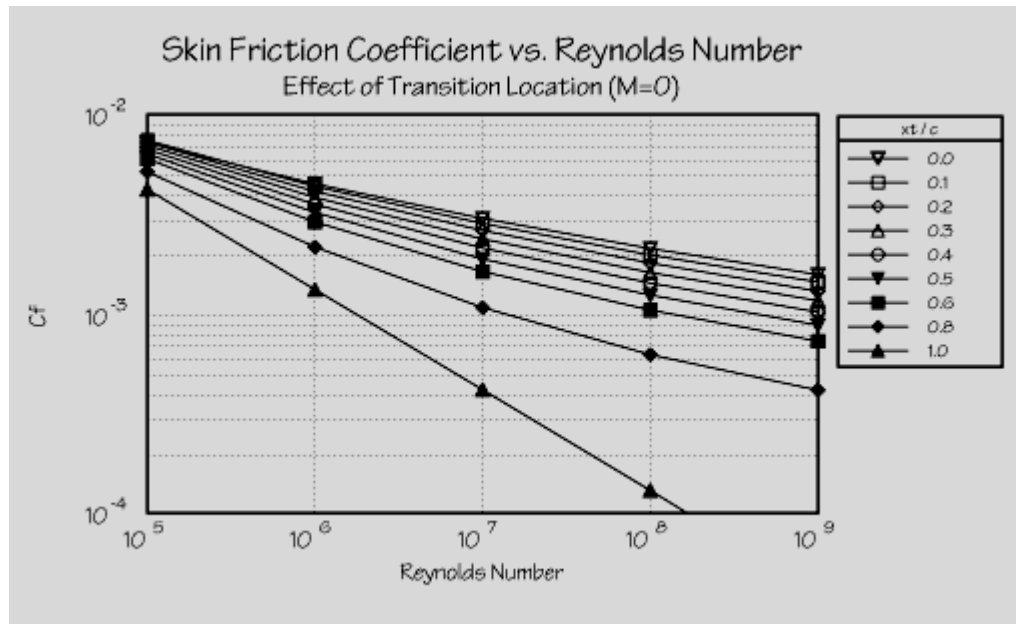
### 2.4.1.1 Skin Friction Coefficient

The skin friction coefficients are sometimes based on experimental data for flat plates with various amounts of roughness. In the present method, experimental results for turbulent flat plates are fit and combined with basic laminar flow boundary layer theory to produce the data in the figure below. The data apply to insulated flat plates with transition from laminar to turbulent flow specified as a fraction of the chord length ( $x_t / c$

= 0 represents fully turbulent flow.) The data are total coefficients; that is, they are average values for the total wetted area of a component based on the characteristic length of the component.



When the skin friction is plotted on a log-log scale the curves are nearly straight lines, but the actual variation of  $C_f$  is more pronounced at lower Reynolds numbers.



For fully-turbulent plates, the skin friction coefficient may be approximated by one of

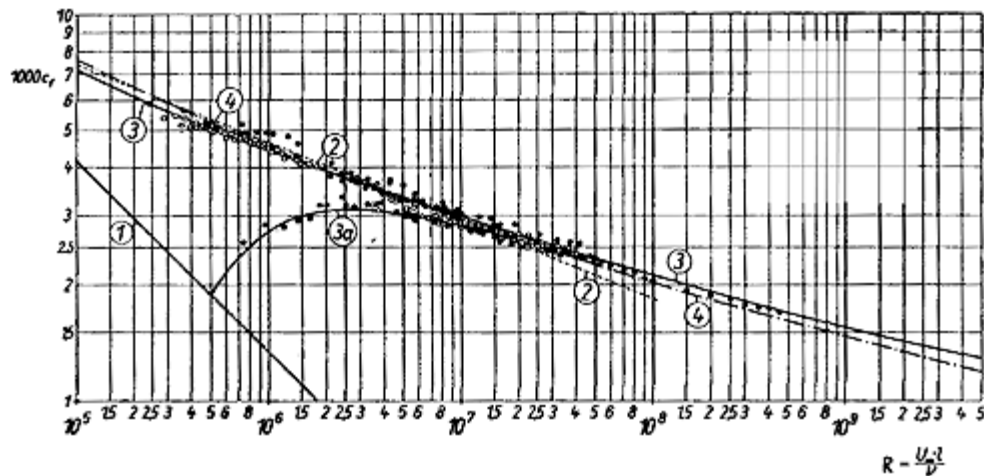


several formula that represent simple fits to the experimentally-derived curves shown in the above figure. For incompressible, flow:

$$c_f = \frac{.455}{(\log Re)^{2.58}} \quad \text{or} \quad c_f = \frac{0.074}{Re^{0.2}}$$

The logarithmic fit by von Karman seems to be a better match over a larger range of Reynolds number, but the power law fit is often more convenient. (Note that the log in the above expression is log base 10, not the natural log, denoted  $\ln$  here.)

In the computation of Reynolds number,  $Re = \rho V l / \mu$ , the characteristic length,  $l$ , for a body (fuselage, nacelle) is the overall length, and for the aerodynamic surfaces (wing, tail, pylon) it is usually the *exposed* mean aerodynamic chord. The values of density ( $\rho$ ), velocity ( $V$ ), and viscosity  $\mu$  are obtained from standard atmospheric conditions at the point of interest. For our purposes we often use the initial cruise conditions. Atmospheric data may be computed in the atmospheric calculator included in the web version of these notes.



Experimental measurements of skin friction coefficient compared with curve fits. Note scatter and transition between laminar and turbulent flow.

### 2.4.1.2 Roughness

It is, for all practical purposes, impossible to explicitly define the incremental drags for all of the protruding rivets, the steps, the gaps, and bulges in the skin; the leakage due to pressurization; etc. Instead, in the method of these notes, an overall mark-up is applied to the skin friction drag to account for drag increments associated with roughness resulting from typical construction procedures. Values of the roughness mark-up factor have been determined for several subsonic jet transports by matching the flight-test parasite drag with that calculated by the method described in these notes. The values so determined tend to be larger for smaller airplanes, but a 6%-9% increase above the smooth flat values

shown in the figure is reasonable for initial design studies. Carefully-built laminar flow, composite aircraft may achieve a lower drag associated with roughness, perhaps as low as 2-3%.

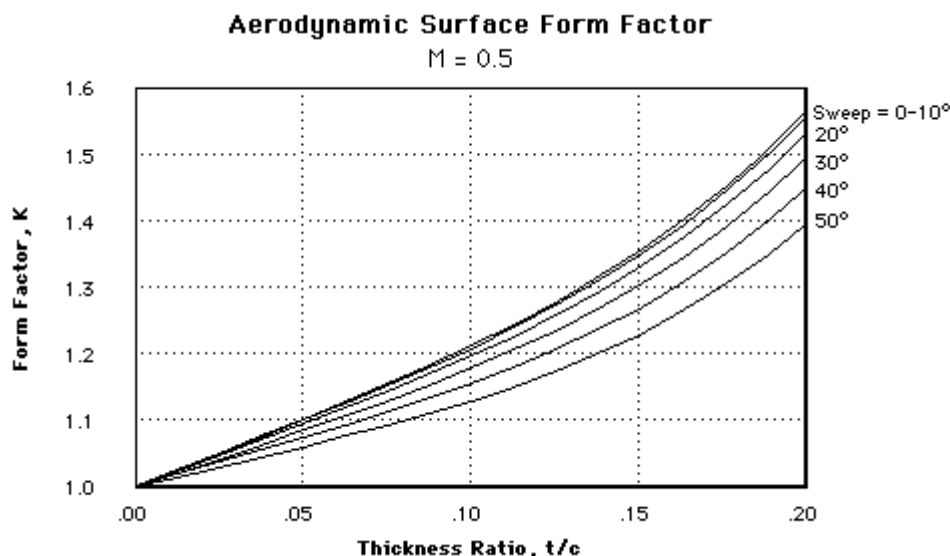
The drag assigned to roughness also implicitly accounts for all other sources of drag at zero lift that are not explicitly included. This category includes interference drag, some trim drag, drag due to unaligned control surfaces, drag due to landing gear door gaps, and any excess drag of the individual surfaces. Consequently the use of the present method implies the same degree of proficiency in design as that of the airplanes from which the roughness drag correlation was obtained.

### 2.4.1.3 Form Factor

The parasite drag associated with skin friction and pressure drag is determined by incrementing the flat plate results by a factor,  $k$ , to account for pressure drag and the higher-than-freestream surface velocities:

$$f = k c_f S_{\text{wet}}$$

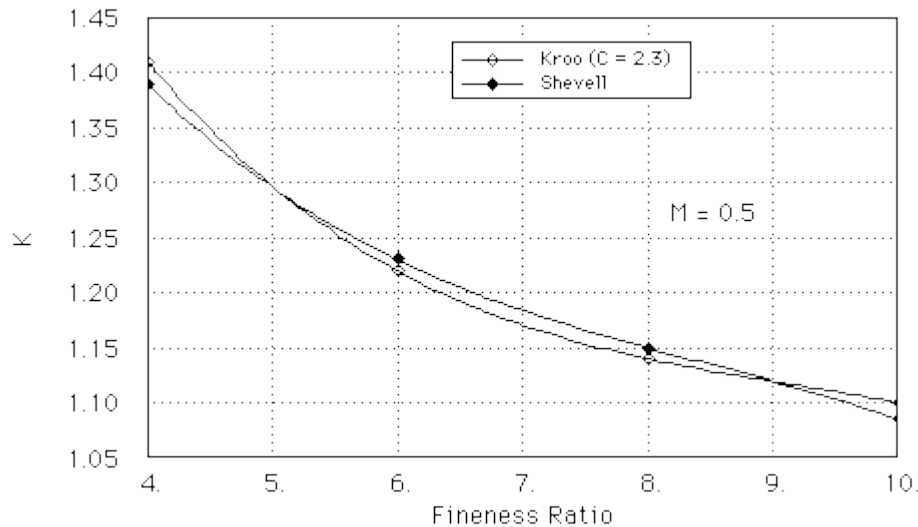
The principal cause of increased drag is the increased surface velocity (supervelocity) due to thickness. For a given airfoil we can compute the maximum increase in velocity. This can also be done for a range of airfoil thickness ratios, wing sweeps, and Mach numbers to determine the form of variation with these parameters. After that one must still resort to experimental data to correlate the actual drag increment associated with skin friction and pressure drag. Such a variation is shown in the figure below at a Mach number of 0.5 for a family of airfoils similar to those used on commercial transports.



The fineness ratio of the fuselage affects the fuselage drag by increasing the local velocities and creating a pressure drag. The increase in skin friction due to higher-than-

freestream velocities can be estimated by considering the symmetric flow around a body of revolution.

For bodies of revolution, the increase in surface velocity due to thickness is smaller than for 2-D shapes. The maximum velocity can be computed as a function of fineness ratio, assuming a family of fuselage shapes. The actual surface velocity distribution depends strongly on the shape of the body: paraboloids have about half again as much maximum perturbation velocity as ellipsoids, and fuselages with constant cross sections are quite different, but the idea here is to represent the correct trend theoretically, and then obtain empirical constants. The results are shown in the following figure.



When the body has a non-circular cross-section, the effective diameter may be computed from:

$$D_{\text{effective}} = (4 S / \pi)^{1/2}$$

where  $S$  is the maximum cross-sectional area.

### 2.4.1.4 Wetted Area Calculations

In order to compute the skin friction drag, it is necessary to multiply this coefficient by the wetted area. For wing-like surfaces, the wetted area is related to the exposed planform area. It is a bit more than twice the exposed area because the arc length over the upper and lower surfaces is a bit longer than the chord:

$$S_{\text{wetted}} \approx 2.0 (1 + 0.2 t/c) S_{\text{exposed}}$$

The exposed area is that portion of the wing planform that is exposed to the airflow. It does not include the part of the wing buried in the fuselage, but does include any chord extensions.

For bodies, the wetted area can be computed by consideration of the actual geometry. This is most easily accomplished with a section-by section analysis and is simplified by CAD programs.

## 2.4.2 Lift-Dependent Drag Items

The total drag coefficient includes the parasite drag and other components:

$$C_D = C_{Dp} + C_{Dvortex} + C_{D\text{lift-dependent viscous}} + C_{D\text{compressibility}}$$

This is sometimes written:

$$C_D = C_{Dp} + C_{Di} + C_{Dc}$$

The second term, is often called the induced drag, but it includes more than just the inviscid drag associated with induced velocities from the wake. For purposes of this analysis, the "induced" drag is customarily divided into viscous and inviscid parts. The inviscid (vortex) drag includes a zero-lift term due to twist, and lift-dependent parts that depend on the twist and planform. The remaining portion of the "induced" drag, the so-called viscous part, is chiefly due to the increase of skin friction and pressure drag with changes in angle of attack. Such increases come about because of the increased velocities on the upper surface of the wing leading to higher shear stresses and more severe adverse gradients with corresponding increase in pressure drag. As in the case of parasite drag, the "induced" drag also includes several miscellaneous effects not accounted for in a simple theoretical study. Additional empirically-estimated terms arise from fuselage vortex drag, nacelle-pylon interference, changes in trim drag with angle of attack, and a change in drag due to engine power effects (either inlet or exhaust).

### 2.4.2.1 Inviscid Part

At low speeds, the inviscid drag of a lifting wing is related to the energy lost in the vortex wake. Simple aerodynamic theory shows that the minimum inviscid drag depends of the span, lift, and speed:

$$C_{Di} = \frac{C_L^2}{\pi AR} \quad \text{or in dimensional terms:} \quad D_i = \frac{L^2}{q \pi b^2}.$$

Simple finite wing theory shows that this result is achieved for planar wings if the distribution of lift over the wing is elliptical. We can make the span loading nearly elliptical with suitable choices of wing planform and twist and so should be able to approach the ideal minimum value quite closely. Generally, twists that are somewhat greater than that required for minimum induced drag are used. This is often done to improve handling or reduce induced drag at low speeds. Thus, the total inviscid drag is somewhat greater than the ideal minimum and is written:  $C_{Di} = C_L^2 / \pi AR e_{\text{inviscid}}$ .

## 2.4.2.2 Trim Drag

When the tail of an airplane carries some load, several drag components are increased: the tail itself has vortex drag and lift-dependent viscous drag, but the lift of the wing must be changed to obtain a specified airplane  $C_L$ :

$$C_{L\text{Airplane}} = C_{L\text{Airplane}} + C_{L\text{tail}} (S_{\text{tail}} / S_{\text{wing}})$$

The increase in wing  $C_L$  means that the wing vortex and lift-dependent viscous drag increases. To compute this, we first must calculate the lift carried by the tail. For most transport aircraft without active controls this is about 5% of the airplane lift, but in the wrong (downward) direction. We could then compute the vortex drag of the combined wing/tail system and then add in viscous and compressibility increments. The difficulty with this is that unless we know the airplane center of gravity (CG) location, we cannot compute the tail load and in the early stages of the analysis, we do not know the airplane CG location. Sometimes we make rough estimates of the CG. When this is not possible, we can rely on more detailed computations done on other aircraft that show trim drag of about 1% to 2% of airplane drag. UAV's with changeable payload can sometimes have larger CG ranges and sometimes, much larger contributions of trim drag.

## 2.4.2.3 Viscous Part

Over most of the flight regime of interest, the viscous part of the "induced" drag may be approximated by a parabolic variation with  $C_L$ . Thus we write:  $C_{Di\_viscous} = K C_{Dp} C_L^2$

Ideally, this drag contribution should be estimated for the individual airplane components, with factors such as the influence of wing leading edge geometry, wing camber, wing thickness ratio, wing sweep, pylon interference, fuselage upsweep, tail induced drag, power effects, etc. taken into account. Since the information required to do this usually does not exist in preliminary design, it is assumed that a new airplane will be similar enough to previous airplanes that the viscous part of the lift-dependent drag can be represented by the equation above, with the K factor determined from previous flight test data. The wing contribution, including the effect of sweep, is included separately from the contributions of the other components. The form of the expression for lift-dependent viscous drag may be derived by combining simple sweep theory with the equation for airfoil superelevations due to circulation.

When each of these effects is added together, the total drag is seen to vary quadratically with  $C_L$ . In fact, apart from the lift dependent twist term, the drag polar is a parabola and would form a straight line when plotted vs.  $C_L^2$ . Since the lift-dependent twist term is usually very small, we expect that the  $C_D$  vs.  $C_L^2$  will be nearly straight. This is often the case. The drag polar can thus be approximated, over most of the range of interest by the two-parameter expression:

$$C_D = C_{Dp} + \frac{C_L^2}{\pi A R e}$$

'e' is a parameter which expresses the total variation of drag with lift. It is sometimes called the span efficiency factor or Oswald efficiency factor after Dr. W.B. Oswald who first used it. It would be 1.0 for an elliptically-loaded wing with no lift-dependent viscous drag, but for practical aircraft 'e' varies from about 0.75 to 0.90.

We can predict the value of 'e' by computing the inviscid drag from a lifting surface method and adding the lift-dependent viscous drag:

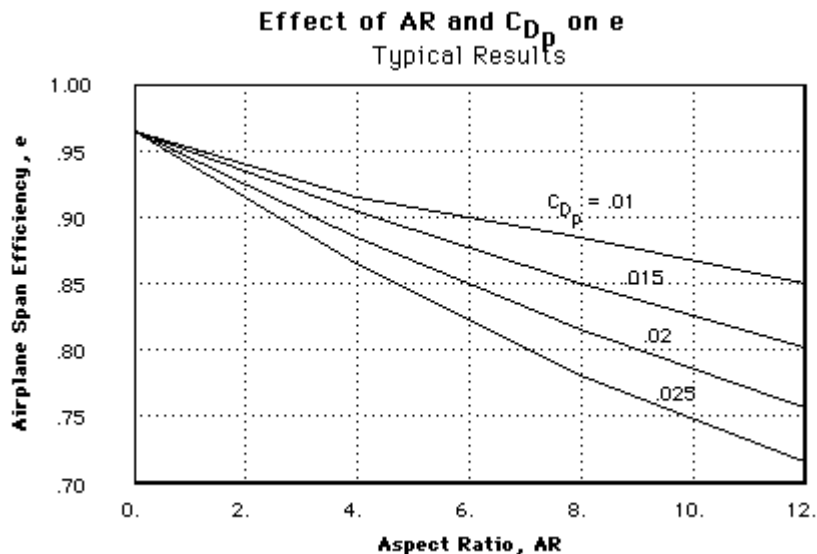
$$C_D = C_{Dp} + C_{Di\_inviscid} + K C_{Dp} C_L^2 = C_{Dp} + C_L^2 / (\pi AR e_{inviscid}) + K C_{Dp} C_L^2$$

So if  $C_D = C_{Dp} + C_L^2 / (\pi AR e)$

then:

$$e = \frac{1}{\pi AR \left( \frac{1}{\pi AR e_{inviscid}} + K C_{Dp} \right)} = \frac{1}{\frac{1}{e_{inviscid}} + \pi AR K C_{Dp}}$$

The figure below shows a typical variation in e with aspect ratio, sweep, and  $C_{Dp}$ . The chart was constructed by assuming  $u = 0.99$  and  $s = 0.975$ , and it works quite well, although the calculation should be done in detail for a specific airplane.  $C_{Dp}$  for jet transports typically varies from about .0140 for aircraft with small ratios of body wetted area to wing wetted area (707 or DC-8) to .0210 for short range aircraft with a relatively large fuselage. The wide-body tri-jets lie in the middle of this range. Small UAV's can have much larger values of  $C_{Dp}$ . **Note that this plot shows typical values; the actual value of 'e' for a particular airplane should be computed as described above.**

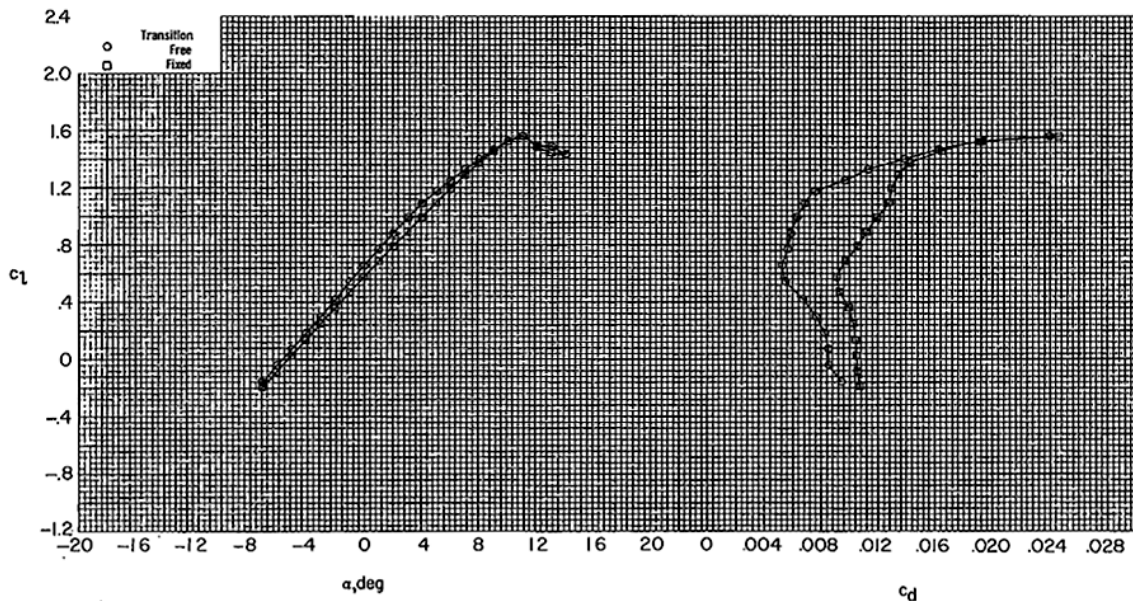


Aircraft with wing-mounted propellers have a further reduction in 'e' due to the downwash behind inclined propellers. The exact effect is difficult to calculate but a reduction of about 4% is reasonable.

## 2.4.3 Improved Method for Wing Drag Build-up

For turbulent wings at high Reynolds numbers and low  $C_L$ , the previous drag build-up method, with constant  $C_{Dp}$  and a quadratic variation in viscous lift dependent drag, works well, but for low Reynolds number wings with laminar flow, or operating near the maximum usable lift coefficient, this approach is very approximate. It is usually better to use more detailed analysis of the wing or airfoil to establish the total viscous-related drag. If the viscous airfoil properties are integrated over the wing and the total established as the wing contribution to  $C_{Dp}$ , then the total drag is closer to:

$$C_D = C_{Dp} + C_L^2 / (\pi AR e_{\text{inviscid}})$$



(a)  $R = 3.0 \times 10^6$ .

Example airfoil data that may be integrated over the wing to compute  $C_{Dp}$  is shown above. Note the different  $C_L$ -dependence of laminar and turbulent data.